Global available solar energy with physical constraints, and associated energy return on investment (EROI)

Elise Dupont[a], Rembrandt Koppelaar[b], Hervé Jeanmart[a]

[a] *iMMC - Institute of Mechanics, Materials and Civil Engineering, Université catholique de Louvain, 1348 Louvain-la-Neuve, Belgium*
[b] *Scene Connect, London N19 4DR, England, UK*

Abstract

The amount of energy striking the earth's surface in one hour is higher than the global annual society's needs, but the fraction of this incoming solar radiation that can sustainably be harvested is greatly constrained by physical, technical and geographical limitations. We argue that the best way to take into account these limitations and to remove any economic bias is to look at the potential with the point of view of net energy analysis. Net energy is the amount of energy that is actually delivered to end-users, after substracting all the energy inputs that need to be invested during the construction, operation, and decommissioning of a facility.

Following our recent work on wind potential, we use a grid-cell approach to assess the theoretical potential of solar energy worldwide. Both photovoltaic (PV) and concentrated solar power (CSP) are considered, with current and next-generation technologies. The study includes land-use constraints, a detailed study of solar-to-electric efficiency with a new parametrisation for CSP, and detailed life-cycle analyses. The final result is the evolution of the energy return on investment (EROI) with the global net potential at global and regional levels.

We find that the global solar potential may be substantially lower than previous estimates, especially when a threshold on the minimum EROI required is applied. The upper limit on the solar potential worldwide was estimated at 1098 EJ/year. 98% of this potential is achievable with an EROI $\geq$ 5, 75% with an EROI $\geq$ 7.5, and only 15% with an EROI $\geq$ 9. Depending on the EROI required to maintain a sustainable society, the achievable potential might be significantly constrained, especially when looking at a regional level, like for example in Europe with only 2% of the global potential.

Keywords: Energy Return on Investment (EROI), PV, CSP, Global potential assessment, Net energy analysis, Life-cycle analysis,

1. Introduction

The negative impacts of fossil fuels on air pollution and climate change, and their limited availability resulting in increasing production costs [1], no longer need to be proven. Yet world fossil fuel consumption continues to increase. In a business-as-usual scenario, various organisations forescast world primary energy demand to grow by 30 % between today and 2040 [2, 3, 4, 5]. The only sustainable scenario is one where renewable energies, mainly wind and solar, supply a large fraction of this increasing energy demand. In contrast, in all of the above studies the share of renewable energies in the energy mix never exceeds 20% to 40% by 2040.

Besides these scenarios based on current and expected policies, possibilities of a 100% renewable energy system by 2050 were investigated [6, 7]. These studies conclude that it is technically feasible to maintain our standards of living and even pursue economic growth with a fully renewable energy system.

Other authors are less optimistic, arguing that 100% renewable energy system scenarios rely on unrealistic or oversimplified assumptions [8]: unrealistic forecasts of energy demand; a belief in technological progress that seems neither technically nor physically possible; a lack of consideration for the intermittency of production and demand-supply matching; and overlooking the structural changes required to adapt the transmission and distribution network. By taking into account physical limits to energy availability and accessibility, they show that today's energy accessibility and availability standards may not be achievable with renewable energies [9, 10, 11].

Hence, whilst there is general agreement that we should urgently move away from fossil fuels and accelerate the transition to a renewable and sustainable energy system, there is no consensus regarding the feasible and desirable pathways to reach it. Given the challenges the world is facing, it is critical to accurately estimate the real potential of renewable energies, mainly wind and solar as their installed capacities are expected to grow manyfold in the coming decades. We have established above that there are large discrepancies in published scenarios of the techno-economic potential of renewable energies. A key reason are imprecise estimates of the physical availability of renewable energy, that result in diverging understandings of how much energy is accessible from the outset, before taking into account implementation speed and intermittency balancing effects.

We believe there is a lack of a sound methodology taking into account physical limits. In this paper we improve upon existing measures of the physical potential of solar following the methodology we developed for wind potential [12], resulting in a physical order of magnitude solar energy value that can be extracted at global and regional levels.

The novelty of the approach is that we assess, for each geographic area, not only the technical potential but also the corresponding amount of energy that will need to be invested in order to produce it. The level of auto-consumption of an energy source is pertinently measured by a dimensionless indicator: the Energy Return On Investment (EROI), calculated for an energy conversion device as the ratio of the energy produced over its lifetime to the energy that was invested, from raw materials extraction to the end-of-life treatment of the facility. Renewable energies are more capital and land intensive than traditional fossil fuels, and as the EROI of fossil fuels decreases with time due to the rarefaction of the resources [13], the EROI of wind and solar facilities will decrease with their spatial expansion [14]. Investment needed for the energy transition is often seen as a great opportunity to create millions of jobs, but if the transition is found to be accompanied with a decrease in the EROI of the energy system, it does mean that in the future we will need more energy to produce our energy. With a decreasing EROI, more and more energy is diverted from other sectors of the economy to feed the energy sector. Based on these considerations, some authors argue that there exists a minimum EROI level necessary to maintain our current level of consumption and way of living [15, 16] and Section 2.1.1. Therefore it is essential to associate to a (potential) renewable energy asset a corresponding EROI level. It will allow to assess whether the new asset will increase or decrease the net available energy to the economy. And thereby enable macro scenario generation to assess whether the structure of the economy, in terms of the size of the energy sector versus the size of other sectors, will dramatically shift during the energy transition.

In Section 2 the state-of-the art and the concepts used in this study are presented. Then the methodology employed is presented in Section 3, followed by the results in Section 4. Finally, the paper ends with a set of conclusions and policy implications in Section 5.

2. Background

This section is divided in two subsections: first the field of net energy analysis is presented.Then the different solar energy conversion technologies are briefly presented, as well as previous studies assessing the global solar energy potential.

2.1. Net Energy Analysis

The transition to renewable energies means a shift from mainly centralised facilities fuelled with high energy density fuels, to a larger share of decentralised facilities powered by intermittent sources (wind and solar radiation). To take into account key limitations to energy harvesting, the field of net energy analysis was developed. The goal is to evaluate to what extent an energy source is able to provide an energy surplus, and as such evaluate the energetic affordability of an energy transformation device. In order to do so, one differentiates between gross and net energy. Net energy produced is the amount of gross energy that remains after substracting the energy that was invested in the energy system, either directly (e.g. direct consumption of ancillary facilities) or indirectly (e.g. during the construction of the site), or both. Indeed, only net energy is actually delivered to end-users and usable for economic activities outside of the energy sector itself. To easily compare different energy sources and their harvesting technologies a dimensionless factor, the energy return on investment (EROI), is used. It is calculated as the ratio of the gross energy produced to the energy invested.

For renewable energy systems, the energy produced depends mainly on the location, while the energy invested in a solar PV panel system or a wind turbine park has limited variability due to globalisation. So, the dominant factor in determining the EROI of a solar PV system or wind turbine system is the location and its solar or wind resource. If we consider that the best sites (better resources, close to the energy users) will be used first, it means that, for a given technological state, the EROI of renewable energies will decrease with their spatial expansion [14, 17]. These authors also showed that technological progress, bounded by physical limits, will not reverse this trend.

2.1.1. The law of minimum EROI

Some studies have shown the correlation between GDP and energy consumption [18], but few research has been conducted on the impacts of energy quality, energy quantity, and EROI levels on economic growth and prosperity, except the work of Lambert et al. [16]. There is a lack of data or knowledge about how EROI would be linked to a society's wellbeing.

The idea behind the theory of the minimum EROI is that any human being needs, in order to survive, to produce more energy than he consumes.

If he is able to produce substantially more than his needs, then he can spend a lot of its time doing other things that producing its energy, like leisure activities for example. If this concept is transposed to a society, it means that the more easily it produces its energy, the more time and energy its citizens are able to spend on consumption activities other than basic needs, and in investments, contributing to economic growth. Following this approach, it might be anticipated that a decrease in the quality of the energy harvested by a society could lead in a decrease of the living standards [15, 19, 16]. The minimum EROI would then be the threshold below which the structure of the economy would dramatically change.
Putting values on this minimum EROI still remains highly speculative. For conventionnal oil, [15] estimates an EROI of 3 would only allow to run transportation, and [19] speculates a minimum EROI of 15 would be needed in order to have access to arts and other leasure activities.

However such estimates do not directly apply to renewable energies. Indeed, renewable energy systems directly produce electricity so they are not constrained by the Carnot limit as fossil fuels are. The electrification of the economy will probably lead to a reduced need in primary energy for similar end-uses (like the use of heat pumps for heating and cooling) [20], and a 100% electrified energy system might be viable with lower EROIs.

Clearly there is a lack of understanding of the potential impacts of a decreasing EROI accompanied by a shift in energy quality, due to a lack of data on one hand but also to a lack of research on the other hand. Given the potential impacts of a decreasing EROI on our living standards, it is important to quantify future EROI scenarios on one hand, while working on this minimum EROI threshold on the other hand.

Static evaluation of the EROI of a particular project or a region are widely present in the literature [21, 22] but few studies estimate a global potential taking account this metric. To our knowledge, the only work that includes EROI considerations in a global model of the future energy system is the work of Dale [23, 24].

Dale modelled the transition to a fully renewable energy system with a global energy model using a biophysical approach. He included dynamic functions for the evolution of the EROI of all energy generation sources (non-renewables and renewables). The EROI functions are calibrated based on historical data and a set of assumptions regarding the availability and assumed past and current EROIs of the different energy sources. The goal of our approach is to focus on these functions and to give them a more realistic

	Total [MW]	**Share [%]**	**PV [MW]**	**CSP [MW]**
World	**295,933**	-	**291,064**	**4,869**
Africa	2,973	1	2,547	425
Asia	139,726	47	139,479	248
Europe	104,590	35	102,282	2,308 (Spain)
North America	37,843	13	36,085	1,758 (USA)
South America	1,974	1	1,974	0
Oceania	5,321	2	5,135	6

Table 1: Installed solar capacity in each continent by the end of 2016 [25]

shape based on a grid-cell approach and detailed life-cycle analyses.

Contrarily to the model of Dale cited above, that includes dynamic estimates of the EROI of different energy sources over a rolling time frame, the approach developed here corresponds to a static evaluation of the EROI of a given worldwide solar potential. The results are therefore representative for solar systems integrated in a fuel based energy system like today's. Further development would be needed in order to dynamically integrate changes in the energy system linked to the energy transition.

2.2. Solar Conversion Technologies

The conversion of the incoming solar radiation into electricity is done by the conversion of light (solar photovoltaic (PV)) or heat (Concentrated Solar Power (CSP)). In this paper we will consider both technologies as they are suitable for different types of solar radiation conditions. Concentrated solar applications need large amount of direct solar radiation, while photovoltaic systems uses both direct and diffuse radiations.

PV systems are currently more competitive than CSP, and dominate the solar energy market. Indeed by the end of 2016 there was almost 300 GW of installed capacity for PV, compared to 4.8 GW for CSP (mainly in Spain and in the United States), see Table 1 and [25]. But as the share of renewables increases, CSP systems will plausibly become more and more attractive. Indeed, because they are easily combined with thermal storage, CSP systems can be designed for base load production (i.e. to provide a constant power output). To provide the same service, PV systems would need to be combined with battery systems of increasing size.

2.2.1. Photovoltaic

As already mentioned, PV systems are the main technology used to convert solar radiation into electricity. Their size vary from residential-scale applications (< 10 kW) to utility-scale applications (several to hundreds of MW). Two types of solar PV modules are common today, poly-crystalline and mono-crystalline silicon, which in 2018 each captured about half of the global market share. They are thus both considered.

2.2.2. Concentrated Solar Power

Concentrated solar power technologies use mirrors or lenses to concentrate direct solar radiations. The concentrated light is transferred as heat to a heat-transfer fluid, the heat is then either stored in insulated tanks or directly used for steam production to generate electricity in a steam turbine. Different technologies exist for the collectors, depending on the way they focus the sun's rays (line or single point) and on the type of heat receiver (mobile or fixed): parabolic through collectors, linear Fresnel reflectors, parabolic dish, and solar power tower. The temperature reached on the receiver depends on the concentration ratio of the collector (i.e. the ratio of the concentrator area to the receiver area). Line focusing systems have typically concentration ratios from 60 to 80 and the receiver temperature reaches 550° C maximum, while single-point receivers reach temperatures of 800° C to 1600° C due to concentration ratios from 600 up to more than 1000.

Parabolic-trough still has the largest market share (85% of the installed CSP capacity) but today the majority of development projects uses the tower-heliostat setup, mainly because at present they can utilise higher temperatures than parabolic-trough. The majority of new plants now also incorporate molten salt based heat storage for up to 12 hours of storage capacity to allow for base-load and load-following operations. Given their relevance today both technologies with and without thermal storage are incorporated in the present study.

2.3. Solar Potential Estimates

A number of studies about global solar potential exist, but results are highly variable (Table 2). The methodology used is most of the time a bottom-up approach. Starting with estimating the area available for solar power plants for each region, with exclusion criteria regarding the land cover type and the level of solar irradiance. Then based on the local average yearly solar irradiance and an estimated actual or projected solar-to-electric conversion efficiency, a technical potential is calculated.

Study	**Technical Potential [EJ/year]**		
	Centralised PV	**Rooftop PV**	**CSP**
Hoogwijk, 2004 [26]	1,300	22	-
Trieb et al., 2009 [27]	-	-	10,605
Global Energy Assessment, 2012 [28]	6,000 - 280,000	-	-
De Castro et al., 2013[29]	60 - 120		
Deng et al., 2015 [30]	316 - 2,815	210	131 - 1,078
Jacobson et al., 2017[6]	41,461	47	31,104

Table 2: Global solar potential estimates

3. Methodology

To derive a more precise estimate of the global solar energy potential, the availability of solar energy is modelled on a net energy basis with a grid cell approach. The same methodology as in our previous work on wind potential [12] is used, which includes the following steps (Figure 1):

1. First a **suitability factor** is associated to each cell, as discussed in Section 3.1, in order to take into account geographical and technical constraints.

2. Then the factors affecting the theoretical **energy outputs** in each cell are discussed and assessed, as described in Section 3.2.

3. With a detailed life cycle inventory, the **energy inputs** for each type of solar plants are evaluated in Section 3.3. The embodied energy calculation was carried out for poly-crystalline and mono-crystalline silicon PV panels, and for two concentrated solar power technologies (parabolic trough and central tower) with varying aperture area and storage size.

4. Based on the findings from Sections 3.2 and 3.3 the EROI of each type of technology is calculated for a given design. The results are straightforward for PV power plants, while for CSP **a model for the evolution of the efficiency** with the level of DNI, aperture area and storage size of the plant was proposed in Section 4.1.1. This parametrisation of the efficiency allows to **optimise the design of CSP power plants** based on the annual DNI of each cell.

5. These results are then combined to derive **estimates of the solar potential and the associated EROI in grid each cell**, as explained in Section 3.4.

The grid size of the model is 0.1° x 0.1° (cells of 100 km^2 on average), which was found to be a good compromise between accuracy and computational effort. The area covered is between latitudes 55°S and 60°N.

3.1. Geographic Suitability Factor

Since many areas are not suitable for solar power applications, realistic assumptions should be taken regarding the available area, accounting for technical and geographical constraints. The solar technology is divided into large-scale applications, i.e. power plants of several megawatts; and small-scale applications, mainly rooftop solar PV panels. The exclusion criteria are different as these two kinds of applications do not compete for the same land area. Indeed large-scale applications require large areas of high solar radiation lands such as deserts, and small-scale applications will be mainly placed on rooftops in urban areas. For centralised applications, we follow the approach that was used for wind potential in [12], i.e. a suitability factor is associated to each grid cell, defined as the cell's fraction suitable for a CSP and a PV solar power plant installation. For rooftop applications, we use the estimates of available rooftop area in each country calculated in [6].

3.1.1. Suitable areas for solar power plants

For centralised applications, we use similar assumptions as in [12], adapted to solar power constraints. Urban areas, bioreserves, and forests are excluded from the analysis, and for other land uses between 5 % to 10 % of global area is considered suitable. Indeed, compared to wind power, solar plants are difficult to combine with other land uses, beyond a few exceptions such as sheep grazing, therefore the suitability factor sould be significantly lower. Land cover of each grid cell was retrieved from the GlobCover 2009 dataset, created by the European Space Agency (ESA) and the Université catholique de Louvain (UCL) which classifies global land cover in 22 classes, at a 10 arc-second resolution [31]. Bioreserves from the world database on protected areas [32] are excluded, as well as relatively remote and unpopulated areas (Antarctica, Greenland and small remote islands). Countries for each grid cell are retrieved from [33].

Finally, exclusion criteria based on terrain slope were applied. CSP plants are not suitable for areas with an average slope greater than 2 % [27, 30], while PV plants may be placed in areas with slopes up to 30 %

Land Cover	Land use factor [%]	Area [10^6 km^2]
Sparse vegetation, grassland, barren areas	10	37
Forests	0	32.4
Croplands	10	7.6
Shrubland	10	8.5
Mosaic vegetation - croplands	5	17.9
Mosaic grassland - forest or shrubland	5	6.9
Urban Areas	0	0.32
Water bodies	0	11.9
Total		**122.5**
Protected Areas	0	17.8
Slope > 2%	0 (CSP)	69.6
Slope > 30%	0 (PV & CSP)	9.4
Suitable for PV plants		**5.4**
Suitable for CSP plants		**2.7**

Table 3: Repartition of the available areas into land use categories and the land use factor for solar power plants, and, for each category, the land use factor for solar power plants.

($\sim$ 16.7°) [30, 34]. The global terrain slope and aspect database from the IIASA was used, which provide 8 classes of terrain slope gradients [35]. 38 % of the onshore area (47 millions km^2) has an average slope $\leq$ 2 %, and 87.5 % of the total area (107 millions km^2) has an average slope $\leq$ 30 %.

The area per land use type and the suitable area for PV and CSP deployment are detailed in Table 3, with the resulting suitability factors presented on a map (Figure 2). The total suitable area per technology was found by combining land use and slope constraints, and by excluding protected and remote areas.

3.1.2. Available rooftop area

For rooftop applications, a common approach is to employ a usability/suitability factor to assess the proportion of the rooftop area suitable for PV panels. This factor limits the total area based on reasonable orientation and little shading. Several methods with varying complexity exist to estimate this factor, as indicated in the review made by the NREL [36].

Detailed estimates of the rooftop area suitable for PV in 139 countries were carried out by Jacobson et al. [6]. They estimated the residential and commercial floorspace available per capita and the fraction of this area that would be technically suitable for PV installation. However the usability factor they applied (in average 65.9 % for residential and 67.2 % for commercial rooftops) is higher than other results from the litterature as assessed by NREL [36]. In this study we use the results from Jacobson et al. [6] for total rooftop area available per country, but we apply a more conservative usability factor of 65 % for commercial rooftops and 25 % for residential rooftops, based on the findings from [36].

3.2. Solar Energy Outputs

To calculate solar power output, a general formula is employed to establish average power produced per unit of area:

$$P = I \cdot \eta \cdot \mathrm{GCR} \quad [W/m^2] \tag{1}$$

With :

- I: the yearly averaged irradiation $[W/m^2]$ (Global Horizontal Irradiation (GHI) for PV and Direct Normal Irradiation (DNI) for CSP).
- η: the conversion efficiency (solar-to-electric).
- ground cover ratio (GCR), the ratio of the active area (the surface occupied by the PV cells or solar collectors) to the ground area (the total ground area occupied by the plant).

These parameters (yearly irradiance, conversion efficiency and ground cover ratio) are detailed in the following sections.

3.2.1. Irradiance

Several freely available datasets exist with yearly average of global horizontal irradiation (GHI) and direct normal irradiation (DNI). In this model we use solar resource data obtained from the Global Solar Atlas, owned by the World Bank Group and provided by Solargis, with a resolution of 30 arcsec (1 km). 8 to 20 years of data were used to estimate yearly averages of daily totals of global horizontal and direct normal irradiation, and the area covered extends from 60° N to 55° S (Figure 3).

3.2.2. Conversion Efficiency

Solar Photovoltaic. The efficiency of solar cells is measured under Standard Test Conditions (STC) : an irradiance of 1 kW/m^2 with a cell temperature of 25° and a solar irradiation angle of 45 degrees, corresponding to a spectrum similar to sunlight hitting the earth's surface at latitude 35° N in the summer. These standard conditions define the nominal power of a photovoltaic panel (expressed in watt-peak, W_p), i.e. an efficiency of 17 % corresponds to 170 W_p/m^2, whereby 1 kW_p would occupy 5.9 m^2. In practice PV panels can produce more power than their nominal power when the irradiance exceeds 1 kW/m^2. The overall efficiency of a PV plant is defined as the product of the efficiency of the solar cells multiplied by a performance ratio. The performance ratio P_r is the ratio of the actual performance of the system to its performance under STC, it includes the optical, array and system losses, and it is independent from the location and the panel orientation. Values typically range between 60 to 90 %, in this study a performance ratio of 81 % is applied as established from tens of thousand of real-life solar systems [37].

On top of that a degradation rate is often included in order to take into account performance decline over time (assumed 0.5 % per year in our calculation [38]). The electricy produced after n years of operation is then calculated as :

$$\begin{aligned} E_n &= \sum_{i=0}^{n-1} \eta_{STC} \cdot p_r \cdot H_{\text{yearly}} \cdot (1-\alpha)^i \\ &= \eta_{STC} \cdot p_r \cdot H_{\text{yearly}} \frac{1-(1-\alpha)^n}{\alpha} \end{aligned}$$

H_{yearly} is the average annual global irradiation (kWh/m^2/year), and α the degradation rate. With a cell efficiency of 17 %, a preformance ratio of 81 % and a degradation rate of 0.5 %, the average efficiency of the system over 25 years would be 13 % (18.6 % for a 24 % efficiency panel).

Concentrated Solar Power. The solar-to-electric efficiency of a CSP plant (i.e. the ratio of the electricity output to the solar irradiance) is the product of the efficiencies of the solar field, of the receiver and of the power block, the latter depending on the temperatures of the steam cycle.

$$\eta = \eta_{\text{field}} \cdot \eta_{\text{receiver}} \cdot \eta_{\text{power block}} \tag{2}$$

The efficiency of the solar field is defined as the ratio of the incoming solar radiation that is transferred as heat to the heat transfer fluid (HTF). It includes optical and geometrical losses (cosine effect, row-to-row shading, and soiling). The receiver efficiency mainly includes thermal losses (for example due to loop piping for parabolic through CSP). In total the thermal efficiency of the solar field has been evaluated around 35-40% [39]. Including the power block efficiency (∼40%, depending on the temperatures reached), the solar-to-electric efficiency is currently around 14-16% for parabolic through, and slightly higher for power tower. This efficiency increases with the level of irradiance: it was estimated at 12 % at 1800 kWh/m^2/year and up to 16 % at 4000 kWh/m^2/year in [40, 41]. Below a certain level of direct solar irradiation, CSP plants do not produce any net electricity because the thermal losses of the receiver and the parasitic consumption of the electric auxiliaries to keep the plant running are almost constant.

Unlike PV plants, where the efficiency does not vary with the size of the installation, the design of CSP plants must be optimised due to the fixed size of the power block. The main parameter to optimise is the total aperture area (total reflective surface), i.e. the optimal number of concentrators (mirros/heliostats) for a given rated power and storage capacity.

First, the area needed to produce the power block rated power at a design point (in general 950 W/m^2 of direct solar irradiance at solar noon on the summer solstice) is estimated, and then a multiplication factor, the solar multiple (SM), is applied to the calculated area in order to take into account lower irradiation levels and storage needs. Typical values for the SM range from 1.3-1.4 (plants without storage) to 2.7 for 12 hours of storage.

$$\text{Aperture Area } [m^2] = \text{SM} \frac{\text{Rated Power [W]}}{\eta_{\text{design}} \cdot \text{DNI}_{\text{design}} [W/m^2]} \tag{3}$$

Therefore, for a given rated power of the power block, the solar multiple is the parameter that must be adapted to the annual average DNI and latitude of a location. According to Eq. (3), the reference area (corresponding to a SM of 1) for a power block of 1 MW and an design efficiency of 22 % would be 4,785 m^2.

Increasing the aperture area above the reference area allows to increase annual production (hence changing the capacity factor), but it also decreases the solar-to-electric conversion efficiency of the plant. Given the fixed power block rating power, oversizing the aperture area increases the risk of curtailment during hours with high direct solar radiation.In addition, increasing the aperture area also increases energy dissipation (thermal losses due to longer pipes for parabolic trough, and optical losses with increasing distance to the receiver for power tower).

In order to model the evolution of the efficiency with the aperture area and location, simulations were run with the System Advisor Model [42] (SAM). For a representative number of locations and solar multiples, the annual energy prodution of CSP plants was estimated and the annual solar-to-electric efficiency was calculated. The simulation results are presented in Section 4.1.1.

3.2.3. Ground Cover Ratio

Utility-scale applications. According to [41, 26] the ground cover ratio is around 20% for PV plants and 13.5% for CSP plants. It means that an entire PV power plant including all infrastructure such as access roads and space for logistics occupies 5 times more space than the effective area of the PV panels. And 7.5 times more space is occupied by a CSP plant relative the area of the concentrating mirrors. To translate this to the model we multiply the available area by the ground cover ratio in order to evaluate the solar potential.

An analysis of existing, under construction and proposed utility-scale facilities in the United States was conducted by the NREL [43]. They estimated total land-use requirements of 32 utility-scale PV plants (a total of 3,751 MW installed) and 22 CSP plants (a total capacity of 1,380 MW of parabolic through projects and 2,358 MW of power tower), and found an average of 19.5% for PV and 15.5% for CSP. These values are similar from previous results for PV, and slightly higher for CSP.

In the model we will use the values proposed by [41].

Rooftop-installed applications. For rooftop applications, this spacing factor is already included in the usability factor described in Section 3.1.2.

3.3. Life Cycle Energy Inputs

Many existing studies calculate the EROI using life-cycle approaches for solar-PV modules, and only a few have studied the EROI of CSP. A meta-analysis for solar-PV was published by [22] and for CSP by [44]. Study results vary due to different boundary and technology assumptions and age of manufacturing input data. We expand upon existing results by taking a complete cradle-to-grave boundary approach, encompassing nine stages from raw materials to final decommissioning, similar to [45], including i) raw materials extraction and conversion to an intermediary material (such as aluminium rolls), ii) transport to the factory, iii) manufacturing of the energy technology and other components, iv) transport to the installation site, v) installation, vi) operation, vii) maintenance, viii) decommissioning, and ix) decommissioning transport. The values thereby include both operational and embodied energy from raw materials extraction and processing.

Data values are presented for 1 GW of 17% efficient polycrystalline silicon photovoltaic power plant (poly-Si-PV), 24% efficient monocrystalline silicon photovoltaic power plant (mono-Si-PV), parabolic trough power plant with oil as HTF (PT-oil), parabolic trough power plant with molten salt as heat transfer fluid (HTF) and 12 hours of thermal energy storage (PT-salt-TES) and solar tower power plant with molten salt as HTF and 12 hours of thermal energy storage (ST-salt-TES). The reference of 1 GW was arbitrarily chosen, and does not reflect the current or expected size of the facilities. All electricity values, except for operational parasitic load, were converted into primary grid inputs, so as to obtain a fuel energy equivalent EROI value, also referred to as primary energy equivalent [46]. The electricity to fuel conversion was carried out by multiplication with a factor of 2.24, indicating that, globally, 2.24 GJ of fuel is required to produce 1 GJ of electricity, as calculated for this study based on the 2015 global electricity mix [47]. This means that the values are representative for solar systems integrated in a fuel based energy system like today's. In contrast a fully 100% renewable scenario study would assume a 1.0 multiplication factor. We will discuss the impact of this factor, and see that its impact on the total energy inputs is relatively limited.

3.3.1. Solar-PV life cycle data

The main components of a solar-PV plant are solar modules, inverters, internal cables and a transformer station. A solar module is composed of solar cells, a film for protection typically made of EVA or Tedlar, glass, an aluminium frame and electronics. Six stages can be distinguished in the production of solar modules, i) extraction of quartz, ii) processing into metallurgical silicon, iii) upgrading to solar grade silicon, iv) manufacturing of wafers from silicon ingots, v) transformation of wafers into solar cells, vi) assembly of solar modules from all components. In addition to these manufacturing stages other phases in the life cycle are included. Table 4 summarizes the energy inputs associated with each stage in the life cycle. The calculation are based on the material needed, the estimated transport distances for each stage, and the energy intensities for materials extraction and transport calculations.

Data is presented firstly for poly-Si-PV based on a 17% efficient solar module, as sold by a majority of manufacturers. It is anticipated that 20% efficient poly-silicon solar module will be on the market within five years based on passivated emitter and rear cell (PERC) designs. Data is secondly presented for mono-Si-PV based on 24% efficient modules, which include hetero-junction mono-silicon with ultra-thin amorphous layers (HJS) [48]. Today, 24% efficient HJS mono-silicon module have been developed by Panasonic and Kaneka. Energy inputs data for metallurgical silicon to silicon modules manufacturing was obtained from recent studies with data from Chinese factories [49] [50]. Data for the additional HJS cell processes, namely amorphous layer deposition PEVCD (plasma enhanced chemical vapor deposition) process and transparent conductive oxide (TCO) sputtering, was taken from [51],[52]. In terms of installation, the most common mounting approach today for solar-PV panels was taken, using galvanized steel based on pile driving, as opposed to concrete ballast systems. Other life cycle material and energy input data was obtained from a recent study by one of the authors with the same nine life cycle stages as adopted in this study [45].

Energy inputs for PV systems are dominated by extraction and processing of minerals (about 60% of inputs), the manufacturing of the solar modules (about 30% of inputs), maintenance (about 7% of inputs), and the operational parasitic load (1% of the outputs). Details are available in the Supplementary Data 5.

About 35% of fixed energy input is electricity that is converted into primary energy based on the earlier 2.24 GJ:1GJ factor. It means that in a fully renewable scenario fixed energy inputs would be reduced by 20%. Fixed energy inputs being those inputs from raw material to decommissioning that are capital related (e.g. as opposed to operational inputs).

3.3.2. CSP life cycle data

Parabolic trough systems are composed of curved solar mirrors usually made out of tempered glass, a HTF pipe system with receiver pipes, and a power plant system. Solar power tower systems are composed of a central tower with a receiver, a field of heliostat flat solar mirrors that focus on the receiver, and a power plant system. Data is presented for three systems, including a PT-oil, PT-salt-TES, and a ST-salt-TES, as outlined in Table 5 (energy inputs for each stage of the life cycle) and in the Supplementary Data 5.

The basic PT-oil without storage is based on an oil HTF system. It represents the until recently commonly installed technology and is based on NREL data for the SAM [53], adjusted to exclude thermal storage. Based on the work of [54] a solar multiple (SM) of 1.3 was taken for the capacity, indicating that the field is slightly oversized relative to the power block.

	poly-Si-PV		mono-Si-PV	
	[GJ/GW]	Share [%]	[GJ/GW]	Share [%]
Raw material extraction & processing	12,211,500	65	8,880,750	55
Raw & intermediary material transport	33,930	0.2	24,660	0.2
Power plant manufacturing	4,394,480	23	5,596,460	35
Construction material transport	303,480	2	218,450	1
Facility construction	71,650	0.4	61,280	0.4
Facility maintenance	1,322,800	7	1,131,300	7
Facility decommissioning	71,650	0.4	61,280	0.4
Decommissioning material transport	315,520	2	226,150	1
Total Energy Inputs [GJ/GW]	18,725,010	100	16,200,320	100
Facility operation [GJ/GJ]	0.0097		0.0097	

Table 4: Summary of life cycle energy inputs for PV technologies.

The ST-salt-TES also utilises the NREL SAM data, which is based on the Ivanpah 377 MW plant in California, USA. The heliostat data for this comes from BrightSource Energy's LH-2.2 heliostat. Storage is based on a tank system with a molten salt mixture including sodium nitrate and potassium nitrate. The system was scaled based on the work of [54] with a SM of 2.7 to account for 12 hours of thermal energy storage (TES), indicating that the field is substantially oversized relative to the power block. A 35% thermal to electric storage efficiency was assumed [55, 56].

The PT-salt-TES represents a next-generation technology. A state of the art trough design is taken based on thin 1 mm steel sheets coated with a reflecting polymer film [57, 58]. The storage system is based on polymer encapsulated phase change salts, which increases thermal conductivity and thus increases energy density and reduces salt storage needs [59], with materials and embodied energy costs taken from [60]. All other components are assumed similar to that outlined in [53]. Similar to the ST-salt-TES a SM of 2.7 and a 35% thermal storage to electricity efficiency is assumed [54, 55, 56].

As the aperture area of the CSP plant is to be optimised in the model (Step 4 in Figure 1), the energy inputs are divided in a fixed part linked to the power block and thermal storage, and a variable part linked to the mirror field.

Energy input data in Table 5 and Supplementary Data 5 are presented for the materials needed for the default aperture area for an installation of 1 GW: 6,22 km^2 for PT-oil and 12,9 km^2 for PT-salt-TES and ST-salt-TES (corresponding to a solar mutiple of 1.3 without storage and 2.7 for 12 hours of thermal storage capacity).

This distinction allows to easily scale up or down the energy inputs for the mirror field, given the optimal aperture area calculated for each location and technology.

The energy inputs for CSP are dominated by extraction and processing of minerals (50% of inputs for installations without storage, up to 70 % with storage), power plant manufacturing (30% of inputs without storage (mainly due to the oil HTF), and 10% with storage), the maintenance (12-15% of inputs), and the operational parasitic load (7% of the outputs). Details are available in the Supplementary data 5.

About 15% of fixed energy input is electricity that is converted into primary energy based on the earlier 2.24 GJ:1GJ factor. It means that in a fully renewable scenario fixed energy inputs would be reduced by 10%.

	PT-oil		PT-salt-TES		ST-salt-TES	
	[GJ/GW]	Share [%]	[GJ/GW]	Share [%]	[GJ/GW]	Share [%]
Raw material extraction & processing	10,775,620	50	30,350,790	70	24,891,800	67
Raw & intermediary material transport	63,650	0.3	116,630	0.3	108,510	0.3
Power plant manufacturing	6,735,420	31	4,412,440	10	3,642,820	10
Construction material transport	517,960	2	1,494,040	3	1,222,840	3
Facility construction	106,000	0.5	220,160	1	220,160	1
Facility maintenance	2,673,540	12	5,511,600	13	5,511,600	15
Facility decommissioning	114,400	1	237,600	1	237,600	1
Decommissioning material transport	630,320	3	1,156,100	3	1,049,220	3
Total Energy Inputs [GJ/GW]	21,616,910	100	43,499,360	100	36,884,540	100
Facility operation [GJ/GJ]	0.073		0.073		0.073	

Table 5: Summary of life cycle energy inputs for CSP technologies.

3.4. Net energy calculation

To retrieve a value for the global solar potential, the solar potential for utility-scale applications and associated EROI will be calculated in each geographical cell for the five technologies presented in Section 3.3. For residential PV applications the results are obtained at a country level, given the availability of rooftop area data.
The net potential in each cell/country is evaluated as follows [14] :

$$\text{Net Energy Produced} = \text{Gross Energy Produced - } \sum \text{Energy Inputs}$$

With gross energy produced calculated based on Eq. (1) using the life time of the facility (25 years for PV power plants and 30 years for CSP power plants), and the energy inputs as evaluated in Section 3.2.

The EROI is calculated as the ratio of gross energy produced to energy inputs, i.e. in cell/country i:

$$\begin{aligned} \text{EROI} &= \frac{\text{Gross Energy Produced}}{\text{Energy Inputs}} \\ &= \frac{\text{Suitable Area}_i \cdot I_i \cdot \eta(I_i, \text{SM}_i) \cdot \text{GCR} \cdot \text{Life Time}}{\text{Energy Inputs(Rated Power, Aperture Area)}} \end{aligned}$$

With the suitable area as evaluated in Section 3.1, I_i the GHI/DNI of the location depending on the technology, and η the solar-to-electric efficiency (depending on the irradiance and solar multiple for CSP applications).

For each technology, a function for the evolution of the EROI with annual production is obtained [14]. The function classifies the sites or countries by decreasing EROI and then draws the evolution of EROI depending on cumulative annual potential. This function aims at providing an upper bound for the EROI associated to a given annual potential. Indeed not only the EROI but also the level of annual potential is important in order to assess the feasability of a solar-powered energetic system.
To retrieve a unique curve for the global solar potential, in each cell the technology is selected that maximises the EROI. The shape of this curve should give a good idea of the repartition of the resources. If, for example, the initial decrease is very steep it would mean that high EROI resources are limited on earth. On the opposite, if there is a large plateau at high EROI values it would mean that many places on earth are suitable for extracting energy from solar radiation at low energy input requirements compared to energy ouput.

This net potential is to be compared with world's final energy consumption, i.e. *the total energy consumed by end users, such as households, industry and agriculture. It is the energy which reaches the final consumer's door* *and excludes that which is used by the energy sector itself [61].* World final energy consumption was estimated around 96 Mtoe(∼400 EJ) in 2016.

4. Results

4.1. CSP design optimisation

By combining the results from the previous sections, the annual energy outputs and associated EROI for each type of solar power plant is estimated for every grid cell. For PV power plants, the results are straightforward as the size of the plant and the amount of solar radiation has a limited impact on the conversion efficiency. However, for CSP plants, the design of the plant (mainly the solar multiple and storage capacity) should be optimised to fit local conditions.

4.1.1. Efficiency model

As previously mentioned, SAM was used to study the impact of the solar mutiple and local radiation on the annual output for the 3 types of power plant described in Section 3.3 (PT-oil, PT-salt-TES and ST-salt-TES). The goal was to establish a relationship for the evolution of the solar-to-electric conversion efficiency with the average DNI of the location and the solar mutliple of the plant (the dependence of the latitude on the efficiency was neglected in our study, as in [27]). In order to do so, 400 representative locations over the world were selected in SAM, and, for each, the annual output of a power plant was simulated for a set of solar multiples, around the values usually applied in existing power plants, which are based on economic evaluations (1.3 without storage and 2.7 with 12 hours of TES).

For each simulation, SAM estimates the annual production of the plant based on hourly resolved irradiance data. The solar-to-electric efficiency is calculated afterwards, based on the average DNI of the location and the aperture area (size of the collector field):

$$\eta_{\text{solar}\to\text{elec}} = \frac{\text{Annual Production } [kWh/year]}{\text{Aperture Area } [m^2] \cdot \text{DNI } [kWh/m^2/year]}$$

To find a regression function for the dependence on DNI and SM, first the evolution of the efficiency with DNI was studied for a fixed value of the SM. The simulation points exhibit a logarithmic dependence of type $\eta = a \ln \text{DNI} - b$, as one can observe in Figure 4.
The parameters a and b were estimated with a least squares linear regression (R^2 between 0.5 and 0.75).

	a_1	a_2	b_1	b_2
PT-oil	-3.38	11.55	23.85	-72.26
PT-salt-TES	-1.578	11.17	10.65	-66.33
ST-salt-TES	-1.62	8.742	11.01	-46.86

Table 6: Parameters for Eq. (4) for each technology, with DNI expressed in kWh/m^2/year.

The evolution of the parameters (a and b) with SM was then studied. The range of SM simulated was from 0.9 to 2 without storage, and from 2.5 to 4 for 12 hours of storage (with a step of 0.1). These ranges were selected in order to remain within realistic designs compared to what is currently done. They exhibit a perfect linear dependence ($R^2 > 0.99$), i.e. a et b are interpolated as linear functions of SM.

The function for the evolution of the efficiency that we proposed in this study is therefore of the following form:

$$\eta(\text{DNI}, \text{SM}) = (a_1 \ \text{SM} + a_2) \ \ln(\text{DNI}) + (b_1 \ \text{SM} + b_2) \qquad (4)$$

With the parameters a_1, a_2, b_1 and b_2 estimated for each technology with a large set of simulations (Table 6).

The efficiency is maximised for low values of the SM. Indeed these configurations allow to convert almost all the incoming solar radiation into electricity. But from an economic point a view they are certainly not optimal as the power block and storage system are underused. From an energetic point of view, the optimal SM is set to maximise the EROI.

4.1.2. EROI maximisation

Thanks to the efficiency parametrisation from SAM simulations, Eq. (4), and with detailed life cycle inputs data from Section 3.3, the EROI of a given CSP power plants is calculated for a given DNI and SM. For each grid cell, the design of a CSP plant is optimised by selecting the SM that maximises the EROI. The optimal SM as a function of the DNI is shown in Figure 5 for the 3 technologies, as well as the SM that maximises the net energy produced per unit of area. We see that these two objectives lead to very different values for the optimal SM. We decided to maximise the EROI of the installation, but we limit the maximum SM allowed in order to remain in realistic designs, and because the efficiency would significantly decrase due to atmospheric attenuation for ST-salt-TES. The maximum was set to 4 for installations with 12 hours storage, this value corresponds to the change in slope in Figure 5, observed because for higher SM there is a lot of curtailment, i.e. a lot of hours when the energy captured by the heliostat exceeds the power block and storage capacity.

As already mentioned, the results indicate that from an EROI point of view it is most of the time better to oversize the heliostat field above what is currently done, even if it slightly decreases the global conversion efficiency due to curtailment and higher losses. Indeed the energetic cost of heliostats is low compared to the power block and storage system, and solar radiation is free, so it is energetically better to optimise the use of the power block and storage system than to maximise the global conversion efficiency. However the EROI criterion does not take into account the area occupied, which is why an upper limit was set to the solar multiple, so as to prevent the model from selecting oversized solar field.

4.2. Technology comparison

Based on the previous calculations, the EROI of the five selected technology systems operating under the same irradiance conditions is compared here. In Table 7 PV panels and CSP facilities are compared in term of area occupied, efficiency, capacity factor, life time energy inputs and outputs, and EROI, with irradiance conditions corresponding to Sevilla, Spain (a yearly averaged GHI of 207 W/m^2, and a yearly averaged DNI of 237 W/m^2).

	poly-Si-PV	mono-Si-PV	PT-oil		PT-salt-TES		ST-salt-TES	
Solar multiple (usual/optimised)	-	-	1.3	1.9	2.7	4	2.7	4
Area occupied [km^2]	29	21	47	68	97	144	102	150
$\eta_{\text{solar}\rightarrow\text{elec}}$ [%]	13	18.6	13	11.9	14.8	13	15.8	14
Capacity Factor [%]	15.8	16.1	19	26	45	59	50	67
Lifetime outputs [PJ]	124.9	126.9	181	242	427	557	478	630
Lifetime fixed inputs [PJ]	18.73	16.2	21.6	27.7	43.5	51.6	36.9	42.6
EROI	7.1	8.2	5.2	5.3	5.7	6	6.7	7
Energy production density [W_e/m^2]	5.4	7.7	4.1	3.7	4.7	4.1	5	4.4

Table 7: Life cycle inputs, outputs and EROI of 1 GW installed for the 5 technologies, with irradiance conditions corresponding to Sevilla, Spain (a yearly averaged GHI of 207 W/m^2, and a yearly averaged DNI of 237 W/m^2).

Among PV technologies, the mono-Si-PV based on the described specifications will always be preferred. Indeed the higher energy inputs needed per unit of area of panels is largely compensated by the extra production thanks to the higher efficiency. Of course, future relative improvements in panel costs of poly vs mono silicon, or the market entry of cheaper solar panels (even with lower efficiencies), could alter this picture. Regarding CSP technologies, the high cost of synthetic oil HTF negatively impacts the EROI of PT-oil compared to PT-salt-TES [62]. ST-salt-TES exhibits the best conversion efficiency for similar energy inputs as PT-salt-TES.

The high capacity factor provided by CSP plants with storage should favor them despite their lower EROI. However, in the model we do not include the capacity factor as a decision variable in the selection of the best technology for each location.

4.3. Global simulation results

4.3.1. Utility-scale potential by technology

The result for the available energy that can be extracted from solar power is presented in this section, based on curves, as described in Section 3.4, with the total net production potential on the x-axis, and the associated EROI on the y-axis.

This resulting function is shown for each type of technology in Figure 6. The potential for CSP is significantly lower than for PV. Indeed the suitable available area is half (due to the slope restriction) and the ground cover ratio is also lower.

The total global net potential for each technololgy was evaluated at 811, 1194, 234, 261, and 294 EJ/year for poly-Si-PV, mono-Si-PV, PT-oil, PT-salt-TES, and ST-salt-TES, respectively. The maximum EROI values are: 9, 10.4, 8.2, 8.5 and 9 for poly-Si-PV, mono-Si-PV, PT-oil, PT-salt-TES, and ST-salt-TES, respectively.

Once the potential is evaluated for each technology separately, the global net potential is calculated by choosing, for each cell, the technology with the highest EROI, see Figure 7. The total global net potential with the best technology in each cell was evaluated at 1098 EJ/year. It is a bit lower than the global potential of mono-Si-PV, because CSP presents better EROI in some cells with high DNI levels, but with a lower production per unit of area due to the ground cover ratio.

We notice that, unlike previous results using a similar methodology for wind energy [12], the decrease in EROI with increasing potential is not particulary steep. 98% of the potential is viable at EROI greater than 5, 75% at EROI greater than 7.5, and 15% at EROI greater than 9. The results indicate that large areas of land are available that also have a good solar resource quality. Indeed the areas with the highest resource (high solar radiation areas like deserts) are in general not suitable for other activities, i.e. thereby suitable for large solar power plants. At a regional level however, there are significant technical solar energy potential differences (see Section 4.4).

Impact of the CSP design optimisation. In Figure 8 the impact of the design optimisation is presented. For each type of CSP technology, the global potential as a function of EROI was drawn, first with the usual and then with the optimal solar multiples (see Table 7). Without storage there is almost no difference as the model will select similar solar multiples than the usual choice. For model runs with 12 hours of storage capacity we notice differences. The curve with the optimal solar multiples presents higher EROIs, but a lower global potential due to the land occupation that increases with a higher solar multiple.

Comparison with previous estimates. The results obtained here can be compared with results from previous studies (Table 2). The global potential obtained is similar to the results from [26], when no restriction is applied on the minimum EROI required, and significantly lower than all the other estimates, except the results for the top-down approach by [29]. The results demonstrate that it is essential to take into account energy input requirements when assessing the available potential of a renewable resource.

4.3.2. Rooftop PV potential

The global potential of rooftop PV is calculated based on the total residential and commercial/governmental rooftop area per country retrieved from [6]. For each country the mean solar irradiance was calculated and used to estimate the production potential per country (See Supplementary Data 5). The global potential, presented as a function of the decreasing EROI in Figure 9, is distributed between residential and commercial rooftops as follows: 28.1 and 28.86 EJ/year for mono-Si-PV, 19.06 and 19.54 EJ/year for poly-Si-PV. With the usability factor applied, the total suitable residential and commercial rooftop areas are very close, hence their potentials are similar.

The resulting value is less than 40 % of the results from Jacobson et al. [6]. They estimated 102.5 EJ/year for residential buildings and 46.7 EJ/year for commercial buildings, despite using the same type of solar panels for the analysis (24 % efficiency panel as the mono-Si-PV). Our results are significantly lower due to more conservative usability factors (see Section 3.1.2) and conversion efficiencies. In the calculation by Jacobson et al., a capacity factor and performance ratio for each country is applied, resulting in an average 19% for the product of the capacity factor and perfomance ratio. In our calculation, with the mean GHI retrieved from the SolarGis database, the average capacity factor is 15 %.

Compared to the power plant potential, the rooftop potential seems marginal: less than 5 % of the global potential for both PV technologies (39 EJ/year compared to 811 EJ/year for poly-Si-PV, and 57 EJ/year compared to 1194 EJ/year for mono-Si-PV). Still it could, theoretically, provide up to 7.5% of the current world's energy needs.

4.3.3. Spatial distribution of the resources

In order to analyse the areas with the highest potential and the areas that would need to be covered with power plants, simulation results are presented on a map of the world using different EROI thresholds (Figures 11 and 12). The applied threshold means that we add a constraint on the minimum EROI required, and all the cells with lower EROIs are excluded. The threshold represents a minimum EROI that needs to be maintained for societies economic balance to continue, without requiring to shift capital from non-energy sectors to energy sector. As already mentined in Section 1, the minimum EROI that a sustainable society must have is difficult to estimate [15, 16]. Here EROI thresholds arbitrarily choosen are presented, to emphasise the decrease in potential when the minimum EROI requirement increases.

A large part of the potential is realised with low EROIs, and when the minimum EROI requirement is increased, only specific regions on earth still possess substantial solar energy potentials.

The technology selected by the model in each cell (i.e. the one maximising the EROI) is represented: areas in blue for PV and areas in orange for CSP.

As previously observed in Figure 7, 98% of the potential is viable with an EROI greater than 5, 75% with an EROI greater than 7.5, and 15% with an EROI greater than 9. Most of the time, PV performs better than CSP, except in very high solar radiation regions (USA, south of Chile and Argentina, south of Australia, and Kazakhstan and Mongolia). When the EROI threshold increases, the fraction of the potential viable with CSP significantly decreases, until eventually there is no CSP left at an EROI

EJ/year	Total	% of Total	PV	% of PV	CSP	% of CSP
Africa	444	40	444	37	112	38
Asia	315	29	361	30	72	25
Oceania	125	11	129	11	55	19
South America	114	10	120	10	23	8
North America	68	6	106	9	25	8
Europe	24	2	27	2	4	1
Total	1099	-	1194	-	294	-

Table 8: Global potential split by continent without an EROI threshold, all values in EJ/year.

threshold of 9. At this EROI level, the only regions where PV is still viable are: Chile, Namibia, a large part of the Sahara, and a small portion of western Australia.

In Figure 12, the results were computed with poly-Si-PV as the unique PV technology. The results differ significantly, since for poly-Si-PV the EROIs of CSP and PV are similar. In contrast to the previous results, CSP is now preferred to PV in Chile, the American Southwest, South Africa, and Australia. And in the last map, showing the available solar potential at EROI ≥ 8 (15% of the global potential), almost no PV is viable.

4.4. Regional potentials

This global potential is further split by continent in Figure 10 and Table 8. As one could expect, there are significant differences between continents. The potential in Africa drives the global curve, as it contains 37% - 40% of the global potential with higher EROI, followed by Asia (25% - 30% of the potential). When we go through the curves from right (Africa) to left (Europe), we notice that the slope of the curve becomes steeper and steeper. The difference of shape between the curve for Africa (almost horizontal) and for Europe (almost vertical) emphasises the uneven distribution of the resources on earth.

In Table 9, we notice that when increasing the EROI threshold to 9, the share of the potential in Africa increases to 67 % of the total (mainly in the Sahara as one can see in Figure 11), followed by 19% in Asia

	Total (PV only)	% of Total
Africa	124	67
Asia	35	19
Oceania	11	6
SouthAmerica	14	8
NorthAmerica	0	0
Europe	0	0
Total	184	

Table 9: Global potential at EROI ≥ 9, split by continent, all values in EJ/year. Table is PV only since the CSP resource potentials viable at this EROI threshold are negligible.

4.4.1. EU-28 countries

Results for the EU-28 countries are shown in Figure 13. The net potentials for each technology was evaluated at 13, 19, 2, 2 and 3 EJ/year for poly-Si-PV, mono-Si-PV, PT-oil, PT-salt-TES, and ST-salt-TES, respectively. The resulting potential is based on the maximum EROI values as follows: 6.8, 7.9, 5.6, 6.3 and 7.4 for poly-Si-PV, mono-Si-PV, PT-oil, PT-salt-TES, and ST-salt-TES, respectively.

As presented in Table 8, the potential in Europe represents only 2% of the global potential. On top of that the EROIs are lower and are decreasing faster, indicating that there are limits to the reliance on solar power to provide a significant part of the European energy needs in the future.

5. Conclusion

Following the work that was done on global available wind energy [12], this study provides a new metholodogy to assess a plausible upper limit for the amount of electricity than can realistically be harvested with solar conversion technologies. Both PV and CSP were included in the analysis, including currently commercialised and next-generation technologies. The study includes land constraints, a detailed study of solar-to-electric efficiency with a new parametrisation proposed for CSP power plants, and a detailed life cycle inventory to establish energy inputs. The final result is an energy potential curve, with the global available solar potential on the x-axis and the corresponding EROI level on the y-axis.

The global net potential (i.e. the amount of energy available after substracting, from the energy produced, the energy invested in order to produce it, both direct and indirect) is as follows:

- PV:
  - Monocrystalline silicon photovoltaic power plant with 24% efficiency: 1194, 1153, 828, and 184 EJ/year, with EROI thresholds of 1, 5, 7.5, and 9, respectively.
  - Polycrystalline silicon photovoltaic power plant with 17% efficiency: 811, 741, 263, and 0 EJ/year, with EROI thresholds of 1, 5, 7.5 and 9, respectively.
- CSP:
  - Parabolic trough power plant with oil HTF: 234, 159 and 1 EJ/year, with EROI thresholds of 1, 5, and 7.5, respectively.
  - Parabolic trough power plant with molten salt HTF and 12 hours of thermal energy storage capacity: 161, 218, and 8 EJ/year, with EROI thresholds of 1, 5, and 7.5, respectively.
  - Solar tower power plant with molten salt HTF and 12 hours of thermal energy storage capacity: 294, 284, and 96 EJ/year, with EROI thresholds of 1, 5, and 7.5, respectively.

Altough many studies conclude that the available solar potential will not be a limiting factor for renewable energy development, this study shows that the energy inputs, i.e. the capital stock, that would have to be mobilised will plausibly require a significant shift from non-energy sectors to the energy sector, with substantial economic impacts, especially when looking at the regional potential for European countries.

Working with EROI as the only decision variable for the choice of a type of technology (i.e. PV or CSP) and the optimal design of a power plant (i.e. the selection of the solar multiple for CSP power plants) has also shown some limitations.

Regarding the type of technology, the model is currently not able to take into account the capacity factor in its selection. While the need for storage remains small under the current global share of renewable energy, it will increase significantly as renewable energies grow in the mix, negatively impacting the EROI [63, 64]. As such, it is not totally fair to compare PV power plants with CSP power plants with 12 hours of TES. In theory, CSP technologies with storage allow for reaching capacity factors close to 100% (with in practice capacity factors around 75% having been attained with such systems), and are therefore more suitable for baseload generation than

PV power plants without storage, whose capacity factors do not exceed 24%. Further analysis would be required to understand the effect of introducing significant battery storage for PV on the global energy potential with EROI constraints. Obviously the inclusion of batteries will decrease the EROI of PV power plants, but the storage capacity needed to reach similar capacity factors as CSP power plants is beyond the scope of this study. Indeed it will require temporally resolved simulations.

Regarding the design of CSP power plants, the EROI maximisation will always select larger aperture areas than what is currently done, until the marginal cost of an additional mirror is higher than the surplus of production generated. This is because there is currently no cost associated to land use. An additionnal constraint linked to the area occupied by power plants should be developed to overcome this limitation.

Regarding the methodology itself, the use of a static approach might be questioned as it does not take into account the evolutions of the energy system accompanying the energy transition. Follow-up research would need to integrate a dynamic approach to take into account the evolution in primary energy needs, but it was beyond the scope of this study.

One might rightly argue that the energy inputs required will decrease with the electrification of the energy system. According to us these improvements will certainly be limited for two reasons:

- the most significant part of the energy inputs are linked to raw materials extraction and processing. It will be difficult to reduce the primary energy needs for the industrial processes needing really high temperatures and;
- the impacts of metal depletion on the cost of extraction of those materials will have a negative impacts on the EROI [65], that is also not taken into account in our static approach.

Further work should combine the results for wind and solar potential so as to better evaluate the extent to which they would be complementary from an EROI perspective. As these two sources of energy are seen as the most promising in order to build a sustainable energy system, this kind of work is essential to build energy scenarios that are based on realistic available resource potentials, especially when informing overarching renewable energy targets in the policy agenda. On top of that, further research is needed on what EROI cut-off level would be sustainable from a societal perspective, and the implications of an energy system falling below this EROI cut-off.

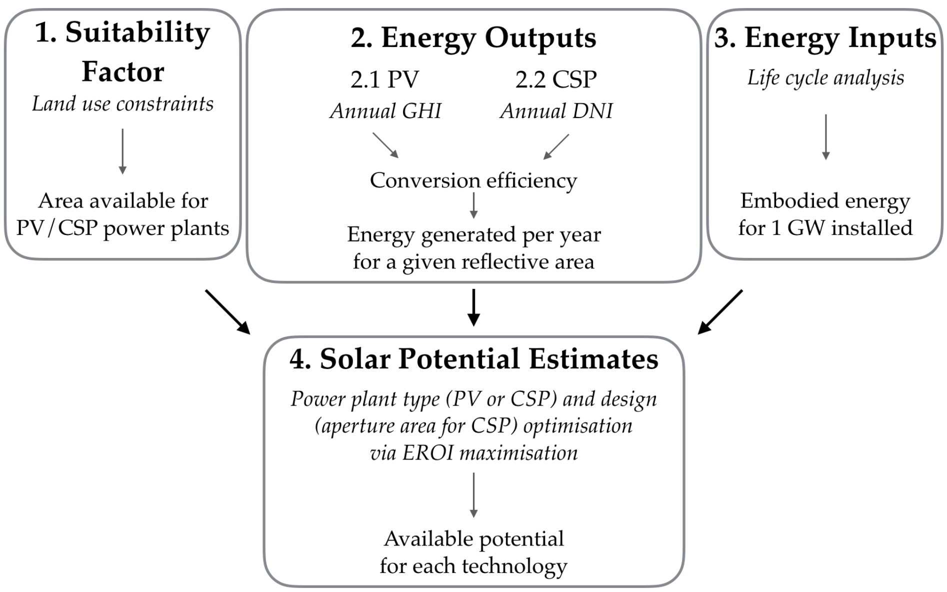

Figure 1: Diagram of the methodology used to evaluate the global available solar potential.

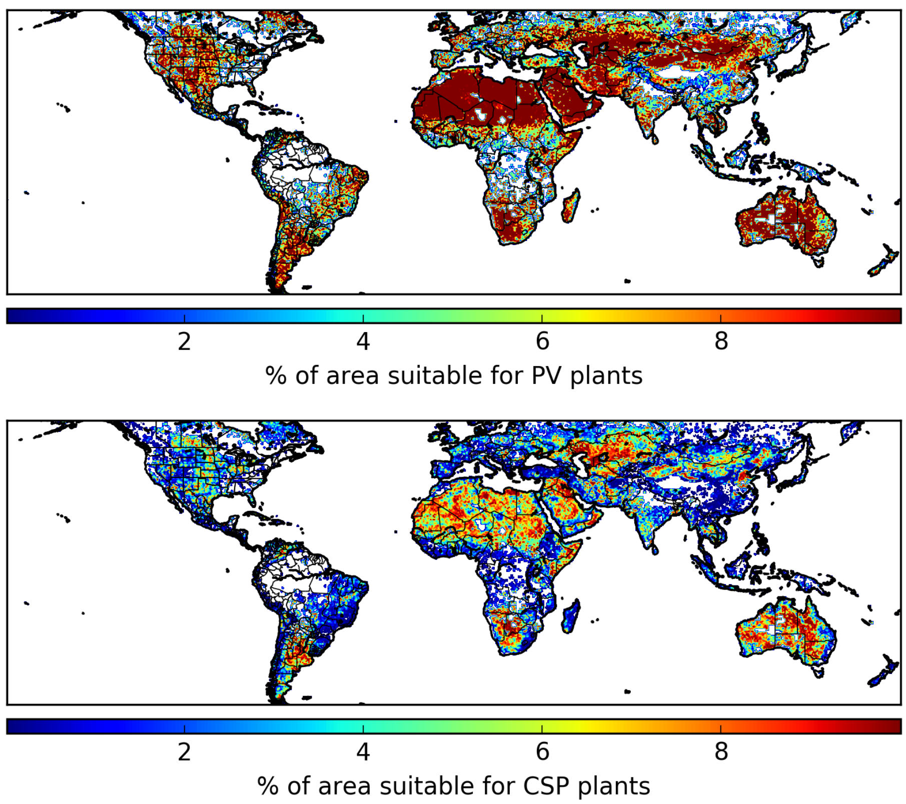

Figure 2: Proportion of the area suitable for centralised solar power plants (from 0 to 10 % of a cell's area).

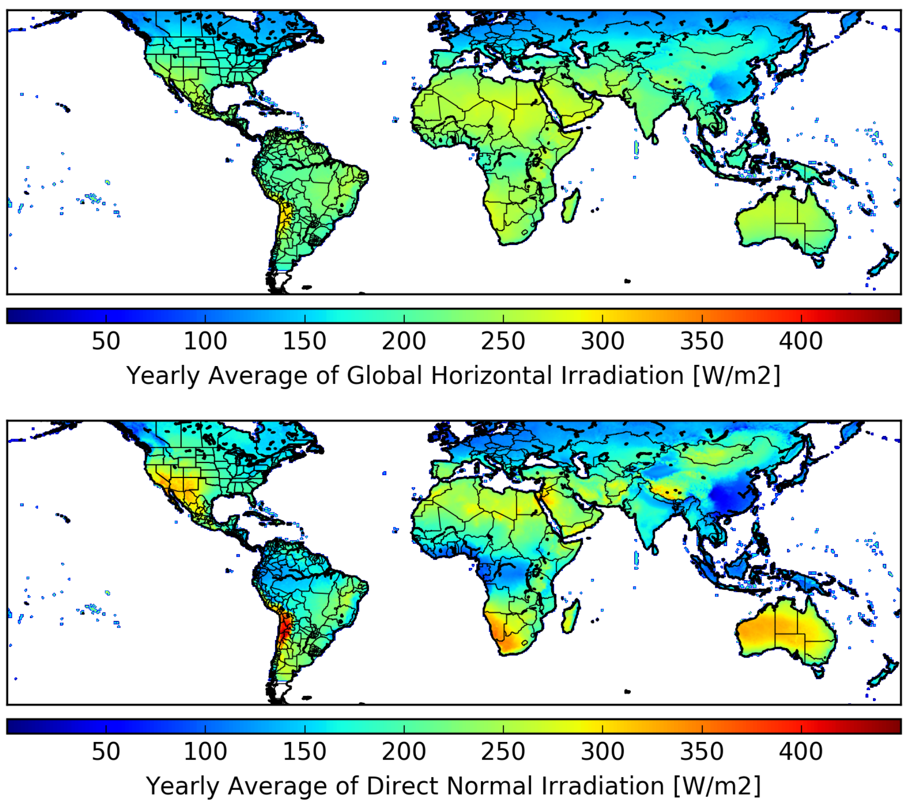

Figure 3: Longterm yearly average of global horizontal irradiation (GHI) and of direct normal irradiation (DNI), data obtained from the Global Solar Atlas, owned by the World Bank Group and provided by Solargis.

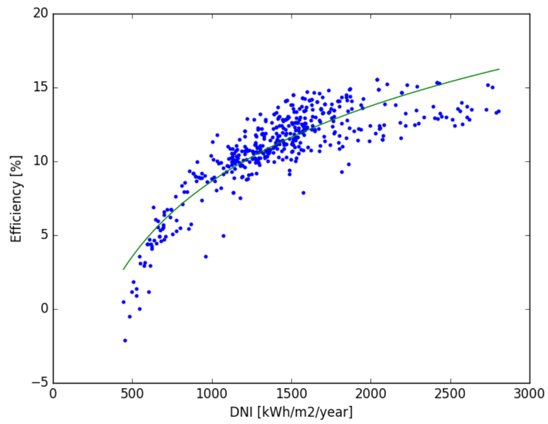

(a) PT-oil, solar mutliple = 1.3

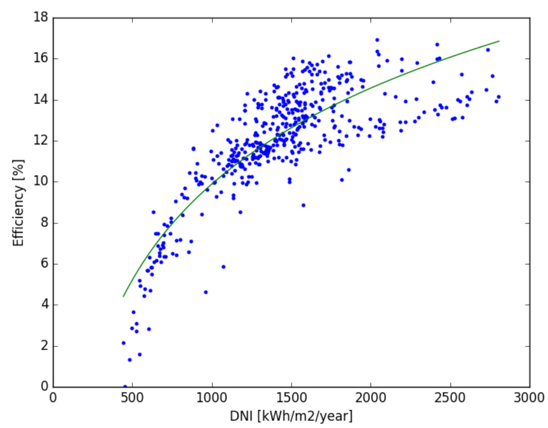

(b) PT-salt-TES, solar multiple = 2.7

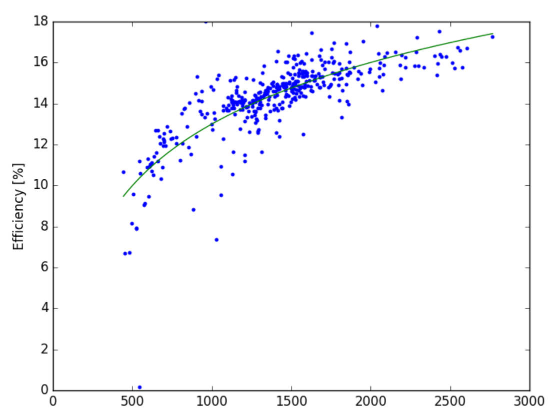

(c) ST-salt-TES, solar multiple = 2.7

Figure 4: Evolution of the efficiency with annual DNI, for PT-oil with a solar multiple of 1.3, and PT-salt-TES and ST-salt-TES with a solar multiple of 2.7, interpolated with the logarithmic function $\eta = 7.349 \ln \mathrm{DNI} - 42.12$, $\eta = 6.747 \ln \mathrm{DNI} - 36.72$, and $\eta = 4.339 \ln \mathrm{DNI} - 16.97$.

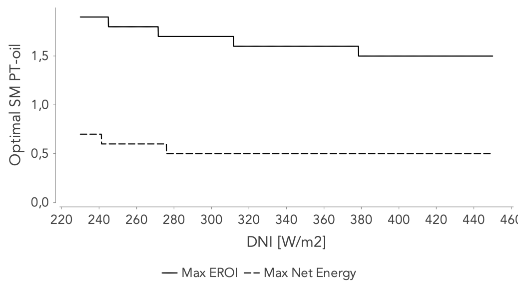

(a) PT-oil

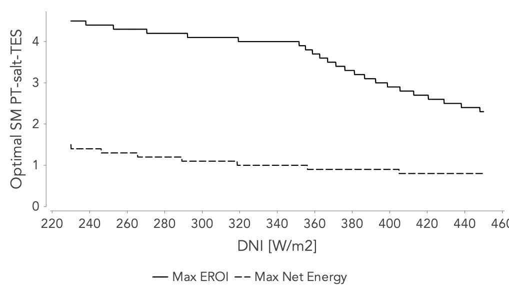

(b) PT-salt-TES

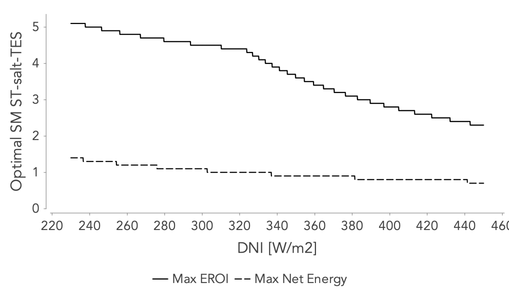

(c) ST-salt-TES

Figure 5: SM maximising the EROI or the net energy production of the installation as a function of the annual DNI.

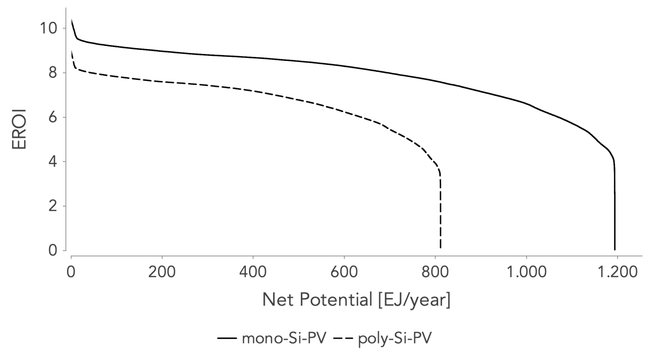

(a) Global potential for the different PV technologies

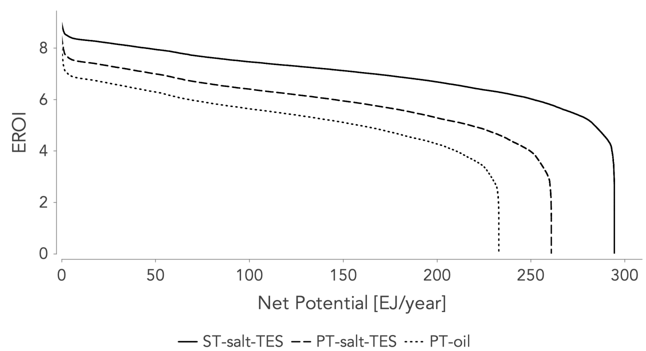

(b) Global potential for the different CSP technologies

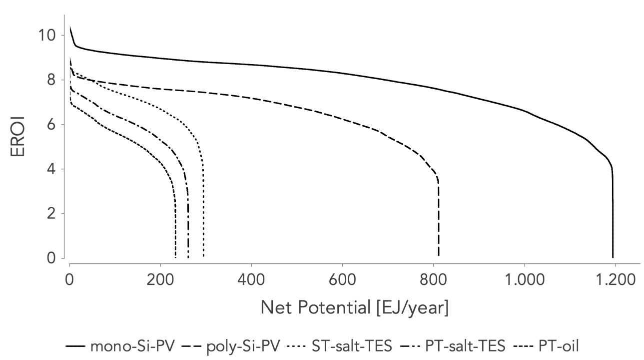

(c) Global potential for all solar technologies

Figure 6: Global solar potential for the different technologies considered in this study.

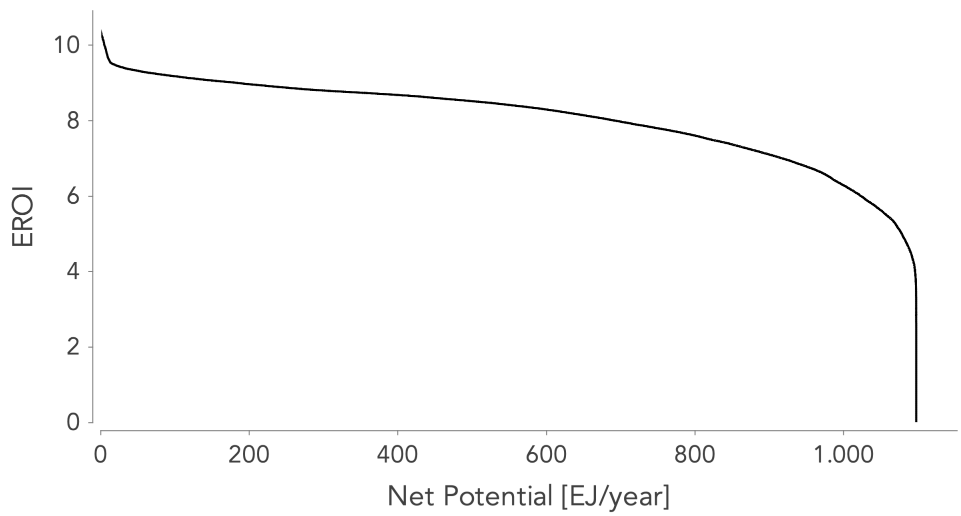

Figure 7: Global solar potential as a decreasing function of the EROI, obtained by selecting the technology with the highest EROI in each cell.

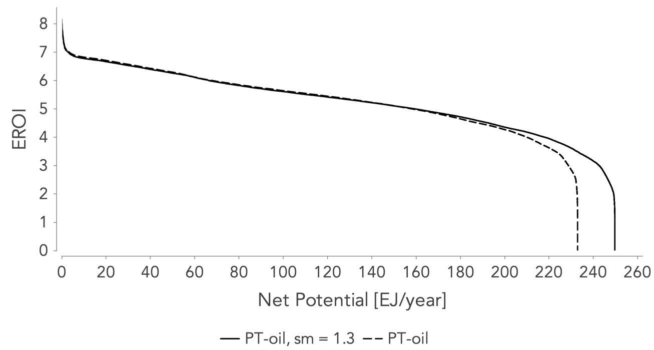

(a) PT-oil

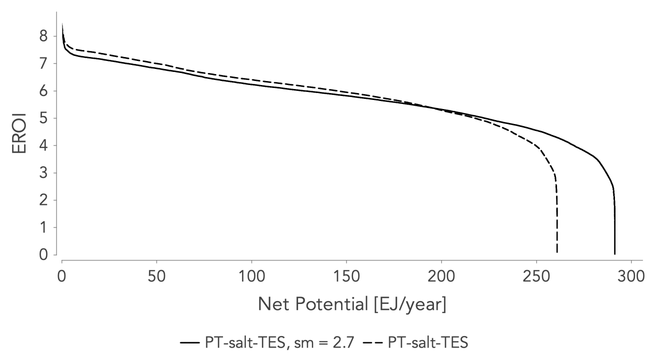

(b) PT-salt-TES

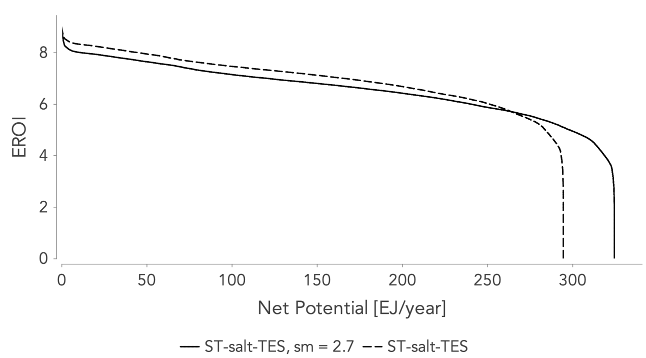

(c) ST-salt-TES

Figure 8: Global potential for each CSP technology, with the usual solar multiple (1.3 without storage and 2.7 with a storage capacity of 12 hours) and with the solar multiple optimised by the model.

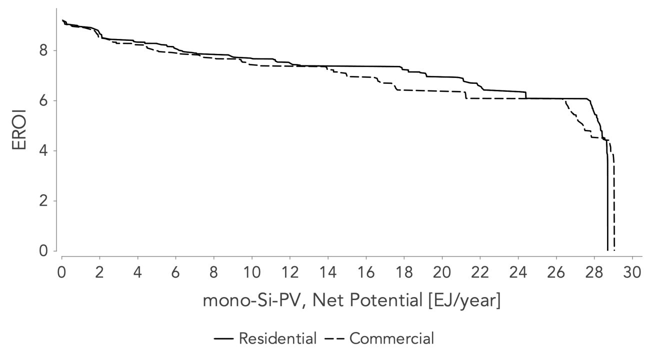

(a) mono-Si-PV

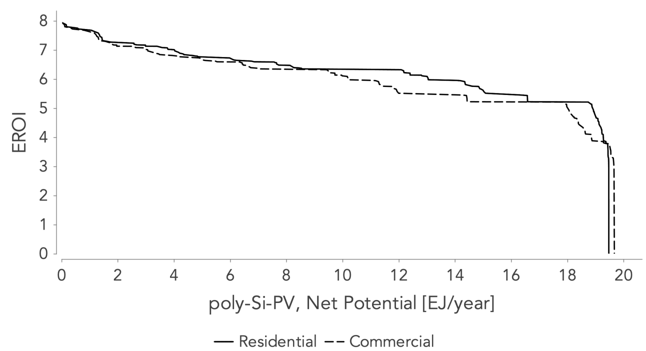

(b) poly-Si-PV

Figure 9: Residential and commercial rooftop PV potentials.

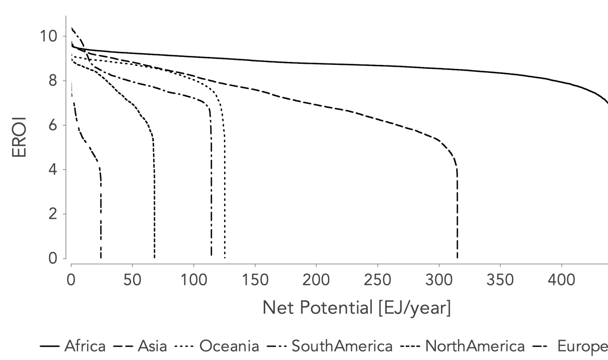

Figure 10: Global solar potential split by continent.

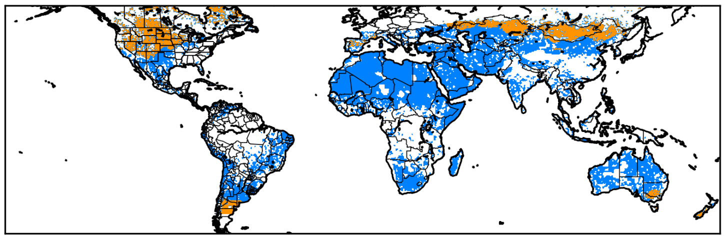

(a) EROI ≥ 5, 98% of the global potential

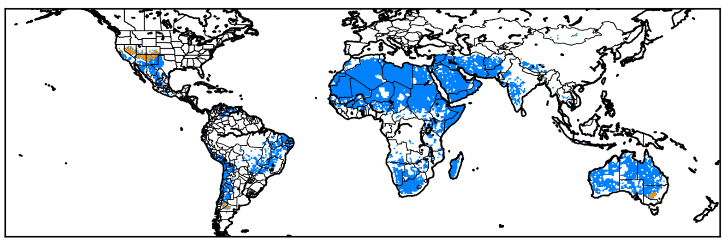

(b) EROI ≥ 7.5, 75% of the potential

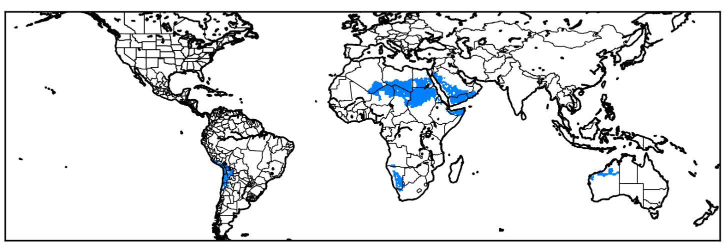

(c) EROI ≥ 9, 15% of the potential

Figure 11: Spatial distribution of the potential, with mono-Si-PV as PV technology. The areas in blue are the areas where mono-Si-PV performs better than CSP, and orange the opposite. The areas with a solar potential are presented for increasing values of the minimum EROI required, from top to bottom.

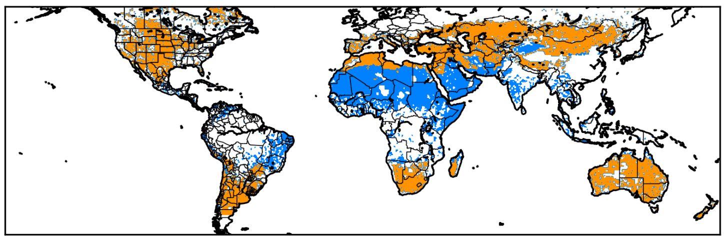

(a) EROI $\geq$ 5, 97% of the global potential

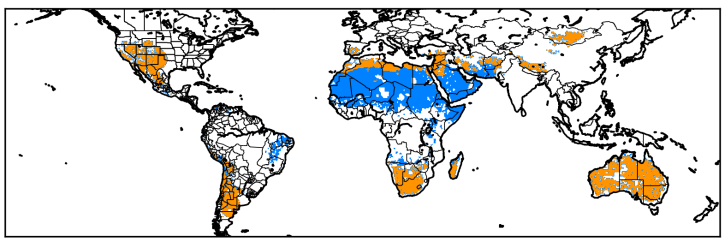

(b) EROI $\geq$ 7, 70% of the global potential

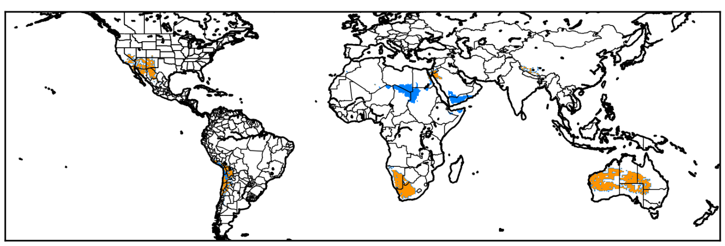

(c) EROI $\geq$ 8, 15% of the global potential

Figure 12: Spatial distribution of the potential, with poly-Si-PV as unique PV technology. The areas in blue are the areas where poly-Si-PV performs better than CSP, and orange the opposite. The areas with a solar potential are presented for increasing values of the minimum EROI required.

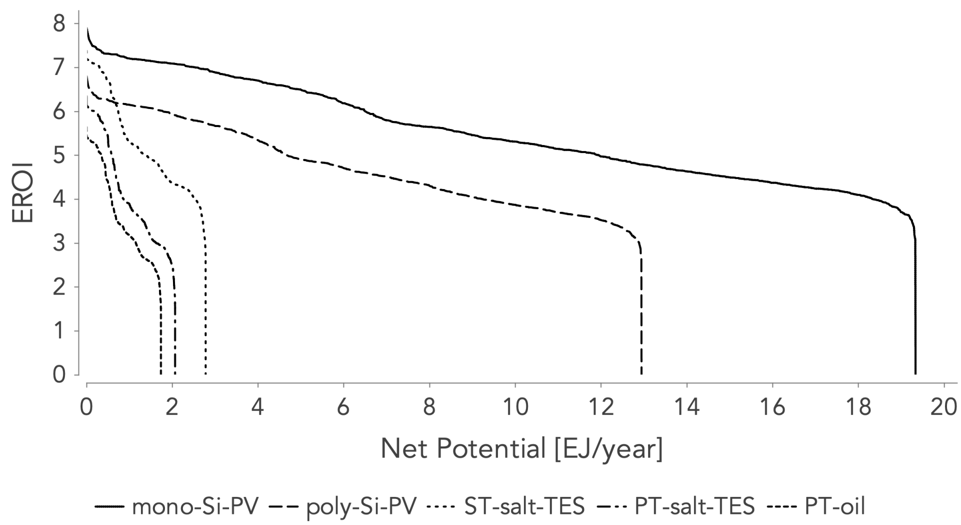

Figure 13: EU-28 countries potential.

Appendix

Supplementary data associated with this article in the attached spreadsheet *Supplementary_Data.xls*.

Acronyms

CSP Concentrated Solar Power.

DNI Direct Normal Irradiation.

EROI Energy Return On Investment.

GCR ground cover ratio.

GHI Global Horizontal Irradiation.

HTF heat transfer fluid.

mono-Si-PV monocrystalline silicon photovoltaic power plant.

poly-Si-PV polycrystalline silicon photovoltaic power plant.

PT-oil parabolic trough power plant with oil as HTF.

PT-salt-TES parabolic trough power plant with molten salt as heat transfer fluid (HTF) and 12 hours of thermal energy storage.

PV solar photovoltaic.

SAM the System Advisor Model [42].

SM solar multiple.

ST-salt-TES solar tower power plant with molten salt as HTF and 12 hours of thermal energy storage.

TES thermal energy storage.

References

[1] Charles A S Hall and John W. Day. Revisiting the limits to growth after peak oil. *Am. Sci.*, 2009.

[2] IEA. World Energy Outlook 2017. Technical report, International Energy Agency, 2017.

[3] WEC. World Energy Focus Annual 2017. Technical report, World Energy Council, 2017.

[4] EIA. International Energy Outlook 2018. Technical report, U.S. Energy Information Administration, 2018.

[5] BP. BP Energy Outlootk 2018 Edition. Technical report, 2018.

[6] Mark Jacobson. 100 % Clean and Renewable Wind , Water , and Sunlight All-Sector Energy Roadmaps for 139 Countries of the World 100 % Clean and Renewable Wind , Water , and Sunlight All-Sector Energy Roadmaps for 139 Countries of the World. *Joule*, 1:108–121, 2017.

[7] WWF. The Energy Report 100 % Renewable by 2050. Technical report, WWF, 2011.

[8] T. W. Brown, T. Bischof-Niemz, K. Blok, C. Breyer, H. Lund, and B. V. Mathiesen. Response to 'Burden of proof: A comprehensive review of the feasibility of 100% renewable-electricity systems'. *Renew. Sustain. Energy Rev.*, 92(September 2016):834–847, 2018.

[9] Patrick Moriarty and Damon Honnery. Can renewable energy power the future? *Energy Policy*, 93:3–7, 2016.

[10] Iñigo Capellán-pérez, Carlos De Castro, and Iñaki Arto. Assessing vulnerabilities and limits in the transition to renewable energies : Land requirements under 100 % solar energy scenarios. *Renew. Sustain. Energy Rev.*, 77(December 2016):760–782, 2017.

[11] Ted Trainer. Some inconvenient theses. *Energy Policy*, 64:168–174, 2014.

[12] Elise Dupont, Rembrandt Koppelaar, and Hervé Jeanmart. Global available wind energy with physical and energy return on investment constraints. *Appl. Energy*, 209(October 2017):322–338, 2018.

[13] Charles A S Hall, Jessica G Lambert, and Stephen B Balogh. EROI of different fuels and the implications for society. *Energy Policy*, 64:141–152, 2014.

[14] Michael Dale, Susan Krumdieck, and Pat Bodger. A dynamic function for energy return on investment. *Sustainability*, 2011.

[15] Charles A S Hall, Stephen Balogh, and David J R Murphy. What is the minimum EROI that a sustainable society must have? *Energies*, 2009.

[16] Jessica G. Lambert, Charles A S Hall, Stephen Balogh, Ajay Gupta, and Michelle Arnold. Energy, EROI and quality of life. *Energy Policy*, 64:153–167, 2014.

[17] Patrick Moriarty and Damon Honnery. What is the global potential for renewable energy? *Renew. Sustain. Energy Rev.*, 16(1):244–252, 2012.

[18] David I Stern. The role of energy in economic growth. *Ann. N.Y. Acad. Sci.*, 1219:26–51, 2011.

[19] Jessica Lambert, Charles Hall, Steve Balogh, Alex Poisson, and Ajay Gupta. EROI of Global Energy Resources Preliminary Status and Trends. Technical Report November, DFID, 2012.

[20] Marco Raugei. Net energy analysis must not compare apples and oranges. *Nat. Energy*, 4:86–88, 2019.

[21] Khagendra P. Bhandari, Jennifer M. Collier, Randy J. Ellingson, and Defne S. Apul. Energy payback time (EPBT) and energy return on energy invested (EROI) of solar photovoltaic systems: A systematic review and meta-analysis. *Renew. Sustain. Energy Rev.*, 47:133–141, 2015.

[22] R H E M Koppelaar. Solar-PV energy payback and net energy : Meta-assessment of study quality , reproducibility , and results harmonization. *Renew. Sustain. Energy Rev.*, 72(August 2016):1241–1255, 2017.

[23] Michael Dale. *Global Energy Modeling: A Biophysical Approach (GEMBA)*. PhD thesis, University of Canterbury, 2010.

[24] M. Dale, S. Krumdieck, and P. Bodger. Global energy modelling - A biophysical approach (GEMBA) Part 2: Methodology. *Ecol. Econ.*, 73:158–167, 2012.

[25] International Renewable Energy Agency. Renewable Energy Statistics 2017. Technical report, 2017.

[26] Monique Maria Hoogwijk. *On the global and regional potential of renewable energy sources*. PhD thesis, Universiteit Utrecht, 2004.

[27] Franz Trieb, Christoph Schillings, Marlene O Sullivan, Thomas Pregger, and Carsten Hoyer-klick. Global Potential of Concentrating Solar Power. In *SolarPaces Conf. Berlin*, pages 1–11, 2009.

[28] GEA. *Global Energy Assessment - Toward a Sustainable Future*. Cambridge University Press, Cambridge, UK and New York, NY, USA and the International Institute for Applied Systems Analysis, Laxenburg, Austria, 2012.

[29] Carlos De Castro, Margarita Mediavilla, Luis Javier Miguel, and Fernando Frechoso. Global solar electric potential: A review of their technical and sustainable limits. *Renew. Sustain. Energy Rev.*, 28:824–835, 2013.

[30] Yvonne Y Deng, Martin Haigh, Willemijn Pouwels, Lou Ramaekers, Ruut Brandsma, Sven Schimschar, and Jan Gro. Quantifying a realistic , worldwide wind and solar electricity supply. *Glob. Environ. Chang.*, 31:239–252, 2015.

[31] ESA and UCL. GlobCover 2009 (Global Land Cover Map). `http://due.esrin.esa.int/page_globcover.php`, 2009.

[32] IUCN and UNEP-WCMC. The World Database on Protected Areas (WDPA). `www.protectedplanet.net/`, 2016.

[33] VLIZ. Union of the esri country shapefile and the exclusive economic zones (version 2). `http://www.marineregions.org/`, 2014.

[34] Carolina Perpiña, Filipe Batista, and Carlo Lavalle. An assessment of the regional potential for solar power generation in EU-28. *Energy Policy*, 88:86–99, 2016.

[35] G. Fischer, F. Nachtergaele, S. Prieler, H.T. van Velthuizen, L. Verelst, and D. Wiberg. Global agro-ecological zones assessment for agriculture. Technical report, IIASA, Laxenburg, Austria and FAO, Rome, Italy, 2007.

[36] J Melius, R Margolis, and S Ong. Estimating Rooftop Suitability for PV: A Review of Methods, Patents, and Validation Techniques. *Natl. Renew. Energy Lab.*, (December):35, 2013.

[37] Jonathan Leloux, Rodrigo Moreton Villagra, Luis Narvarte Fernandez, Jamie Taylor, David Trebosc, and Adrien Desportes. Monitoring 30,000 PV Systems in Europe: Performance, Faults, and State of the Art. In *31st Eur. Photovolt. Sol. Energy Conf. Exhib.*, number September, pages 1–21, 2015.

[38] D. C. Jordan and S. R. Kurtz. Photovoltaic degradation rates - An Analytical Review. *Prog. Photovoltaics Res. Appl.*, 21(1):12–29, 2013.

[39] CSP Bankability. Draft for an Appendix C – Solar Field Modeling to the SolarPACES Guideline for Bankable STE Yield Assessment. Technical Report 0325293, 2017.

[40] IEA. Technology Roadmap Concentrating Solar Power. Technical report, International Energy Agency, 2010.

[41] IRENA. Estimating the Renewable Energy Potential in Africa A GIS-based approach. Technical report, International Renewable Energy Agency, 2014.

[42] NREL. System advisor model 2014.1.14. `https://sam.nrel.gov/`, 2017.

[43] S. Ong, C. Campbell, P. Denholm, R. Margolis, and G. Heath. Land-Use Requirements for Solar Power Plants in the United States. Technical Report June, 2013.

[44] John J. Burkhardt, Garvin Heath, and Elliot Cohen. Life Cycle Greenhouse Gas Emissions of Trough and Tower Concentrating Solar Power Electricity Generation: Systematic Review and Harmonization. *Journal of Industrial Ecology*, 16(SUPPL.1), 2012.

[45] Zoltán Kis, Nikul Pandya, and Rembrandt H.E.M. Koppelaar. Electricity generation technologies: Comparison of materials use, energy return on investment, jobs creation and CO2emissions reduction. *Energy Policy*, 120(May):144–157, 2018.

[46] V. M. Fthenakis, R. Frischknecht, M. Raugei, H. C. Kim, E. Alsema, M. Held, and M de Wild Scholten. Methodology Guidelines on Life Cycle Assessment of Photovoltaic Electricity. *Methodology Guidelines on Life Cycle Assessment of Photovoltaic Electricity*, IEA PVPS T(5454):International Energy Agency Photovoltaic Power Sys, 2011.

[47] British Petroleum. BP Statistical Review of World Energy. Technical report, BP, 2016.

[48] Y. Ohshita, T. Kamioka, and K. Nakamura. Technology Trends of High Efficiency Crystalline Silicon Solar Cells. *AAPPS Bulletin*, page 7, 2017.

[49] Guofu Hou, Honghang Sun, Ziying Jiang, Ziqiang Pan, Yibo Wang, Xiaodan Zhang, Ying Zhao, and Qiang Yao. Life cycle assessment of grid-connected photovoltaic power generation from crystalline silicon solar modules in China. *Applied Energy*, 164:882–890, 2016.

[50] Zhiqiang Yu, Wenhui Ma, Keqiang Xie, Guoqiang Lv, Zhengjie Chen, Jijun Wu, and Jie Yu. Life cycle assessment of grid-connected power generation from metallurgical route multi-crystalline silicon photovoltaic system in China. *Applied Energy*, 185:68–81, 2017.

[51] A. Louwen, W.G.J.H.M. Sark, R.E.I Schropp, W.C. Turkenburg, and A.P.C. Faaij. Life-cycle greenhouse gas emissions and energy payback time of current and prospective silicon heterojunction solar cell designs. *Progress in Photovoltaics*, 23:1406–1428, 2015.

[52] A. Louwen. *Assessment of the energy performance , economics and environmental footprint of silicon heterojunction photovoltaic technology.* PhD thesis, University of Utrecht, 2016.

[53] Craig Turchi, Parthiv Kurup, Sertac Akar, Francisco Flores, Craig Turchi, Parthiv Kurup, and Sertac Akar. Domestic Material Content in Molten-Salt Concentrating Solar Power Plants Domestic Material Content in Molten-Salt Concentrating Solar Power Plants. *Nrel/Tp-5500-64429*, (August), 2015.

[54] Jennie Jorgenson, Paul Denholm, Mark Mehos, and Craig Turchi. Estimating the Performance and Economic Value of Multiple Concentrating Solar Power Technologies in a Production Cost Model. (December), 2013.

[55] Justin Raade, Travis Starns, Cam Martin, Ron Hanson, and Jon Lagarenne. Utilizing Molten Salt Energy Storage at Thermal Power Plants Halotechnics , Inc . – Corporate Profile. pages 1–19, 2015.

[56] Craig Turchi. Concentrating Solar Power : Current Cost and Future Directions. 2017.

[57] Skyfuels ReflecTech. ReflecTech White Paper: Embodied Energy. Technical report, 2009.

[58] Nathan Schuknecht, Jennifer Mcdaniel, and Harrison Filas. Achievement of the $ 100 / m 2 Parabolic Trough. In *SolarPaces 2017 , 26-29 September, Santiago, Chile*, page 8 pages, 2017.

[59] A. Mathur, R. Kasetty, J. Oxley, J. Mendez, and K. Nithyanandam. Using encapsulated phase change salts for concentrated solar power plant. *Energy Procedia*, 49:908–915, 2013.

[60] Rhys Jacob, Martin Belusko, Ines A. Fernandez, Luisa F. Cabeza, Wasim Saman, and Frank Bruno. Embodied energy and cost of high temperature thermal energy storage systems for use with concentrated solar power plants. *Applied Energy*, 180:586–597, 2016.

[61] Eurostat. Eurostat, 2018.

[62] E. Batuecas, C. Mayo, R. Díaz, and F. J. Pérez. Life Cycle Assessment of heat transfer fluids in parabolic trough concentrating solar power technology. *Sol. Energy Mater. Sol. Cells*, 171(May):91–97, 2017.

[63] Gauthier Limpens and Hervé Jeanmart. Electricity storage needs for the energy transition: An EROI based analysis illustrated by the case of Belgium. *Energy*, 152:960–973, 2018.

[64] Ted Trainer. Estimating the EROI of whole systems for 100 % renewable electricity supply capable of dealing with intermittency. *Energy Policy*, 119(May):648–653, 2018.

[65] Florian Fizaine and Victor Court. Renewable electricity producing technologies and metal depletion: A sensitivity analysis using the EROI. *Ecol. Econ.*, 110:106–118, 2015.